

DOE/NASA/16310-15  
NASA TM-103727

# **Tensile Behavior of Tungsten/Niobium Composites at 1300–1600 K**

Hee Mann Yun  
Cleveland State University

and

Robert H. Titran  
National Aeronautics and Space Administration  
Lewis Research Center

Work performed for

**U.S. DEPARTMENT OF ENERGY**  
**Office of Nuclear Energy**

Prepared for the  
Fall Meeting of the Metallurgical Society  
Indianapolis, Indiana, September 30—October 6, 1989

## DISCLAIMER

This report was prepared as an account of work sponsored by an agency of the United States Government. Neither the United States Government nor any agency thereof, nor any of their employees, makes any warranty, express or implied, or assumes any legal liability or responsibility for the accuracy, completeness, or usefulness of any information, apparatus, product, or process disclosed, or represents that its use would not infringe privately owned rights. Reference herein to any specific commercial product, process, or service by trade name, trademark, manufacturer, or otherwise, does not necessarily constitute or imply its endorsement, recommendation, or favoring by the United States Government or any agency thereof. The views and opinions of authors expressed herein do not necessarily state or reflect those of the United States Government or any agency thereof.

Printed in the United States of America

Available from

National Technical Information Service  
U.S. Department of Commerce  
5285 Port Royal Road  
Springfield, VA 22161

NTIS price codes<sup>1</sup>

Printed copy:

Microfiche copy: A03

<sup>1</sup>Codes are used for pricing all publications. The code is determined by the number of pages in the publication. Information pertaining to the pricing codes can be found in the current issues of the following publications, which are generally available in most libraries: *Energy Research Abstracts (ERA)*; *Government Reports Announcements and Index (GRA and I)*; *Scientific and Technical Abstract Reports (STAR)*; and publication, NTIS-PR-360 available from NTIS at the above address.

## **Tensile Behavior of Tungsten/Niobium Composites at 1300-1600 K**

Hee Mann Yun  
Cleveland State University  
Cleveland, Ohio 44115

and

Robert H. Titran  
National Aeronautics and Space Administration  
Lewis Research Center  
Cleveland, Ohio 44135

Work performed for  
U.S. DEPARTMENT OF ENERGY  
Office of Nuclear Energy  
Washington, D.C. 20545  
Under Interagency Agreement DE-AI03-86SF16310

Prepared for the  
Fall Meeting of the Metallurgical Society  
Indianapolis, Indiana, September 30—October 6, 1989

# TENSILE BEHAVIOR OF TUNGSTEN/NIOBIUM COMPOSITES AT 1300 TO 1600 K

Hee Mann Yun  
Cleveland State University  
Cleveland, Ohio

and

Robert H. Titran  
National Aeronautics and Space Administration  
Lewis Research Center  
Cleveland, Ohio

## Abstract

The tensile behavior of continuous-tungsten-fiber-reinforced niobium composites (W/Nb), fabricated by an arc-spray process, was studied in the 1300 to 1600 K temperature range. The tensile properties of the fiber and matrix components as well as of the composites were measured and were compared to rule of mixtures (ROM) predictions. The deviation from the ROM was found to depend upon the chemistry of the tungsten alloy fibers, with positive deviations for ST300/Nb (i.e., stronger composite strength than the ROM) and negative or zero deviations for 218/Nb.

## LIST OF SYMBOLS

$\sigma_{PL}$	proportional limit
$\sigma_{PL,f1}$	proportional limit of fiber 1
$\sigma_{PL,f2}$	proportional limit of fiber 2
$(\sigma_{PL})_C$	proportional limit of composites
$(\sigma_{PL})_{cal}$	calculated proportional limit of composites
$(\sigma_{PL})_{exp}$	experimentally measured proportional limit
$\sigma_f$	tensile stress of the fiber
$\sigma_m$	tensile stress of the matrix
$V_f$	volume fraction of the fiber
$V_m$	volume fraction of the matrix
$G_f$	shear modulus of the fiber
$G_m$	shear modulus of the matrix
$\Delta\sigma_m$	matrix strengthening
$\sigma_{M,m}$	Brown's mean stress
$\sigma_C$	composite strength
$\sigma_C^*$	composite strength calculated by the modified ROM
$\sigma_C^{exp}$	composite strength measured experimentally
$\sigma_C^{ROM}$	composite strength calculated by the ROM
$\epsilon_1$	strain at the yield point of fiber 1
$\epsilon_2$	strain at the yield point of fiber 2
$\epsilon_p$	accumulated plastic strain

## Introduction

Continuous fiber reinforced metal matrix composites are attractive materials in applications where high strength at high temperatures is desired. The high-temperature stability of these composites is believed to be superior to that of discontinuous fiber composites. In addition, the mechanical properties of axially reinforced composites can be modeled easily because of the uniform distribution of an externally applied load in a plane normal to the fiber direction. The rule-of-mixture (ROM) method generally can be used to predict the mechanical behavior of composites, if we make two assumptions: (1) that no shear stress is transferred from the matrix to the fiber, and (2) that the strain is distributed homogeneously between the fiber and matrix (Ref. 1).

TABLE I. - CHEMICAL COMPOSITION OF COMPOSITE CONSTITUENTS (at %)

Materials	ThO <sub>2</sub>	K	W	Nb	O	C	N
	at %						
ST300	<sup>b</sup> 1.0	-----	balance	-----	-----	-----	-----
218	-----	<sup>b</sup> 0.38	balance	-----	-----	-----	-----
Nb	-----	-----	-----	balance	<sup>a</sup> 0.27	<sup>a</sup> 0.11	<sup>a</sup> 0.041

<sup>a</sup>Trace elements O, C and N were analyzed after arc-spraying of niobium wires to form the composite matrix.

<sup>b</sup>Taken from (Ref. 6).

A limitation to the use of the ROM has been observed in room-temperature tensile properties of tungsten and copper composites, where residual stresses (Refs. 2 and 3), matrix strengthening (Ref. 4), and lateral stresses (Ref. 4) were observed, resulting in a deviation from the ROM prediction. At high temperatures, the deviation may be greater, and the mechanisms causing it more complicated. In the present study, tungsten fiber reinforced niobium matrix (W/Nb) composites were tested in tension in the temperature range 1300 to 1600 K. Results were evaluated using the ROM and interpreted in terms of fiber degradation and/or matrix strengthening.

### Experimental Procedures

#### Materials

Table I shows the chemical compositions of the constituents examined in this work. The 218 wire is strengthened by potassium-filled bubbles, and the ST300 wire is strengthened by 1.0 at % thoria. Both wires were purchased in the "cleaned and straightened" (CS) condition with a nominal diameter of 200  $\mu\text{m}$ . All of the unidirectional fiber composite materials, as well as the unreinforced niobium (Nb) matrix material, tested in this study were fabricated using an arc-spray process with uniform processing parameters (Ref. 5).

#### Mechanical Property Testing

Pin and clevis thin-sheet specimens (Fig. 1) with the longitudinal direction parallel to the fiber axis were made from composite panels by electric discharge machining (EDM). Tungsten reinforcing tabs were electron-beam welded onto the specimen ends (Fig. 1) to prevent pin pull-out during testing. Tensile testing of the sheet specimens was conducted in a vacuum of about  $10^{-5}$  Pa at temperatures from 1300 to 1600 K. Tensile property measurements were carried out in a universal testing machine operated at crosshead speeds of 0.00085 to 0.85 mm/sec. This would correspond to strain rates of  $3.3 \times 10^{-5}$  to  $3.3 \times 10^{-2}$  sec<sup>-1</sup>, based upon the assumption that deformation took place only in the 25.4 mm-gauge section. Tensile strength of the wires was measured on the as-drawn and electropolished wires. Details of the wire tensile tests were described previously (Refs. 5 and 6). Due to the high temperature and high vacuum it was not possible to use an extensometer to measure strain. Therefore, the tensile strengths and proportional limits were determined from load versus time curves.

## Results

### Tensile Behavior of Tungsten-Niobium Composites and of Niobium Matrix Material

Figure 2 shows the stress-displacement behavior of the composite and the niobium matrix specimens tested at 1600 K at three different crosshead speeds. The fiber volume fraction of the composites varied from 0.31 to 0.33 as determined by counting the number of fibers during metallographic examination of the specimen cross sections. For ease of comparison, tensile stress values throughout this report were normalized to a constant fiber volume fraction of 0.33 by the simple relationship,  $\sigma_c = (\sigma_c' / V_f') \times V_f$ , where  $\sigma_c$  is the normalized stress at the  $V_f$  value of 0.33, and  $\sigma_c'$  and  $V_f'$  are the measured actual stress and fiber volume fraction, respectively. The actual displacement value in the gauge section is

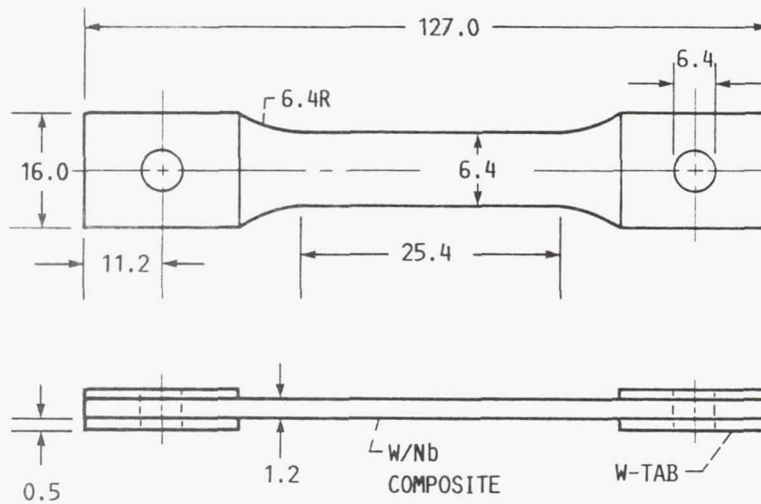


FIGURE 1. - SHEET SPECIMENS USED FOR TENSILE TESTING OF COMPOSITE PANELS AND ARC-SPRAYED SHEET. DIMENSIONS IN MM.

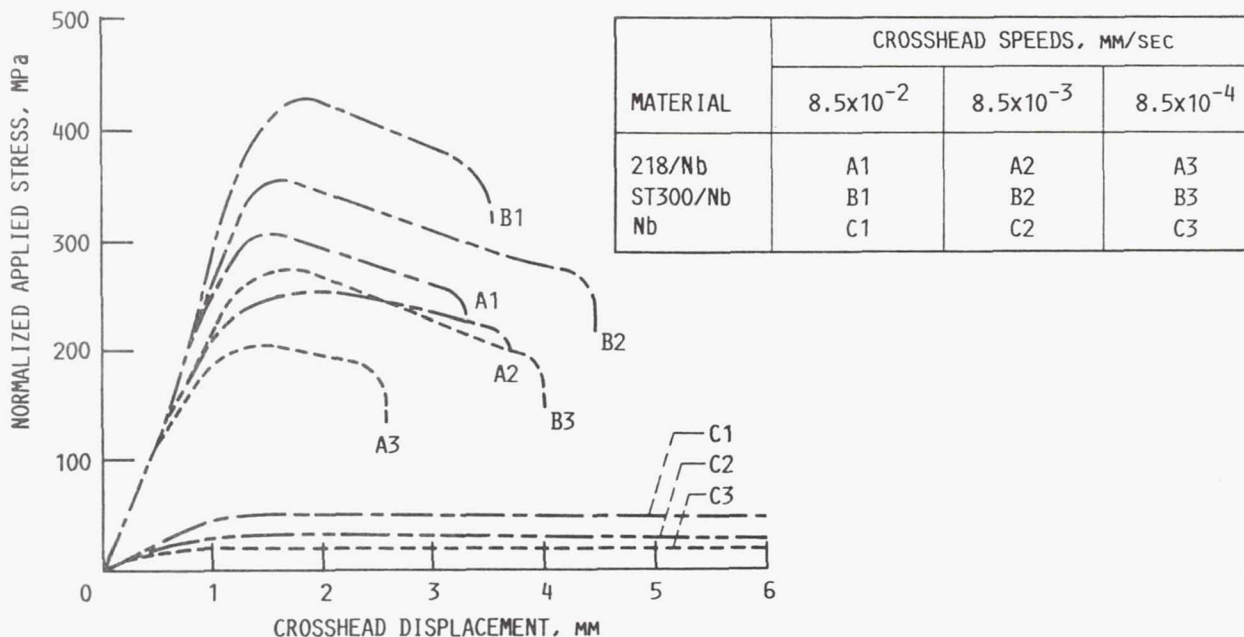


FIGURE 2. - STRESS-DISPLACEMENT BEHAVIOR OF COMPOSITES AND ARC-SPRAYED NIOBIUM TESTED AT 1600 K. THE APPLIED STRESSES WERE NORMALIZED TO 33 FIBER VOLUME PERCENT.

believed to be somewhat smaller than the calculated value due to deformation outside the gauge section. This implies that the stress increment in the elastic region should be higher.

In Fig. 2, the niobium matrix material showed relatively low strength and elastic deformation, but exhibited a longer plastic deformation region than the W/Nb composites, with a nearly constant flow stress at 1600 K. The ST300/Nb composites had larger elastic deformation, higher proportional limit ( $\sigma_{PL}$ ), higher ultimate tensile strength (UTS) and a larger fracture deformation than the 218/Nb composites. In the plastic region, the composites exhibited smooth strain hardening with about a 100 MPa increase from the proportional limit to the maximum stress. The composites also have a relatively long plastic deformation region between maximum stress and fracture. This behavior is believed indicative of good bonding between the fiber and matrix. The  $\sigma_{PL}$  and UTS for 218/Nb, ST300/Nb and Nb are shown in Fig. 3 as functions of crosshead speed at

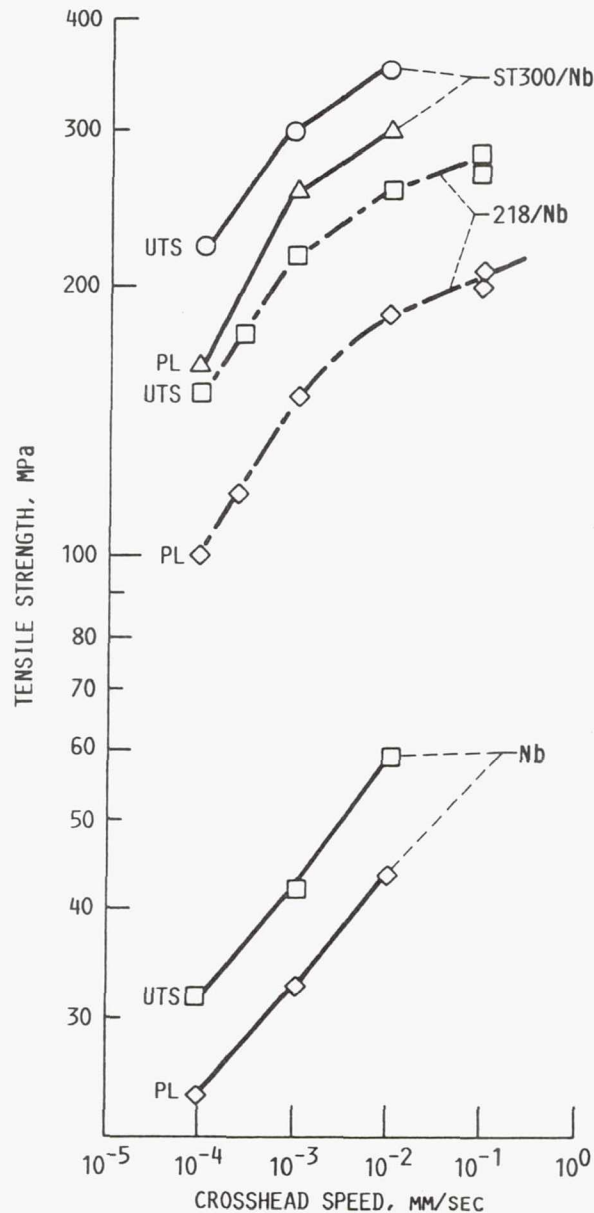


FIGURE 3. - UTS AND PROPORTIONAL LIMIT AS A FUNCTION OF CROSSHEAD SPEED AT 1600 K. DATA POINTS FOR THE TENSILE STRENGTH OF COMPOSITES ARE NORMALIZED TO 33 FIBER VOLUME PERCENT.

1600 K. The effect of crosshead speed on the tensile properties was considerably high. At this high temperature, the tensile strength increased by almost a factor of two as the crosshead speed increased.

The  $\sigma_{PL}$  and UTS for 218/Nb, ST300/Nb and Nb are shown in Fig. 4 as a function of temperature. The tensile strength of the ST300/Nb composites are observed to be substantially higher than the 218/Nb composites over the entire temperature range. The UTS value of Nb at 1600 K is about 30 MPa. Fiber reinforcements with 218 or ST300 tungsten increased the UTS to about 200 and 280 MPa, respectively.

#### Tensile Behavior of Tungsten Wires

The tensile strength of 218 and ST300 tungsten wires, as-drawn and electropolished, is shown in Fig. 5 as a function of temperature. The ST300

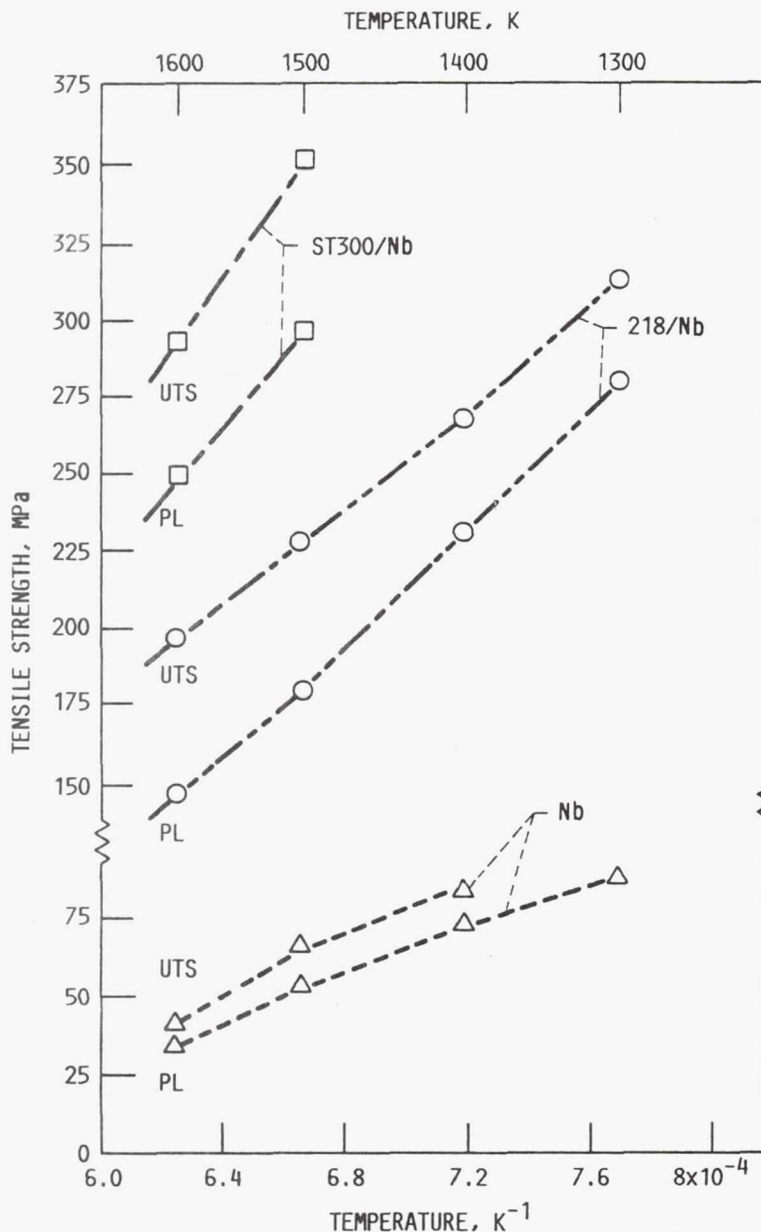


FIGURE 4. - TEMPERATURE DEPENDENCY OF TENSILE STRENGTH OF 218/Nb, ST300/Nb AND Nb, TESTED AT A CROSSHEAD SPEED OF  $8.5 \times 10^{-3}$  MM/SEC. DATA POINTS FOR THE TENSILE STRENGTH OF COMPOSITES ARE NORMALIZED TO 33 FIBER VOLUME PERCENT.

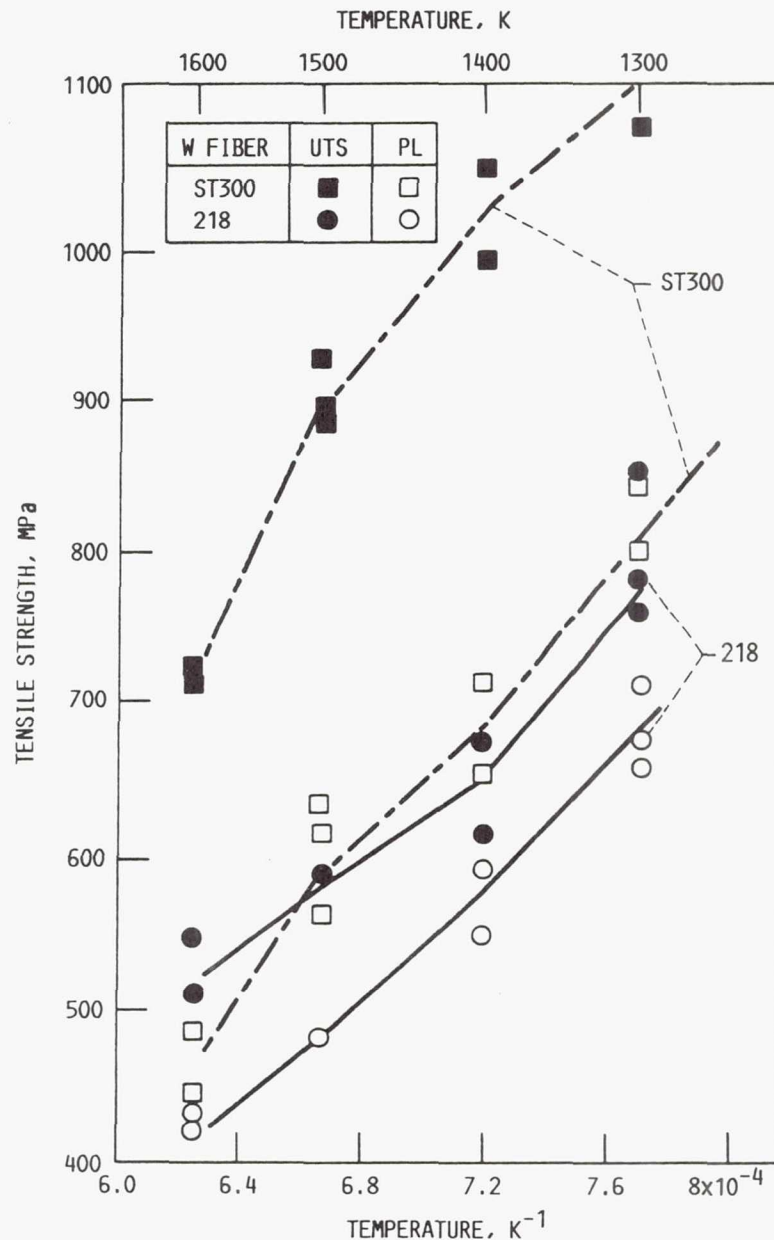


FIGURE 5. - TEMPERATURE DEPENDENCY OF TENSILE STRENGTH OF 218 AND ST300 TUNGSTEN FIBER FROM [6], TESTED AT A CROSSHEAD SPEED OF  $8.5 \times 10^{-3}$  MM/SEC.

tungsten wires showed higher tensile strength than the 218 tungsten wire, especially below 1500 K. The tensile strength difference between the two wires becomes smaller, as the testing temperature increased from 1500 to 1600 K.

#### Interaction Between Fiber and Matrix

Longitudinal and transverse sections of tensile tested specimens were examined metallographically. Transverse sections were cut perpendicular to the fiber and the tensile load axis; longitudinal sections were cut parallel to the fiber and the specimen face. Longitudinal sections were prepared by polishing until the approximate center of the fiber in the middle layer of the three fiber layer composite was evident. Figure 6 shows the results of scanning electron microscopy of 218 and ST300/Nb composites in the as-fabricated condition and after tensile testing. Both 218 (Fig. 6(c)) and ST300 fiber components (Fig. 6(d)) displayed considerable segmentation and

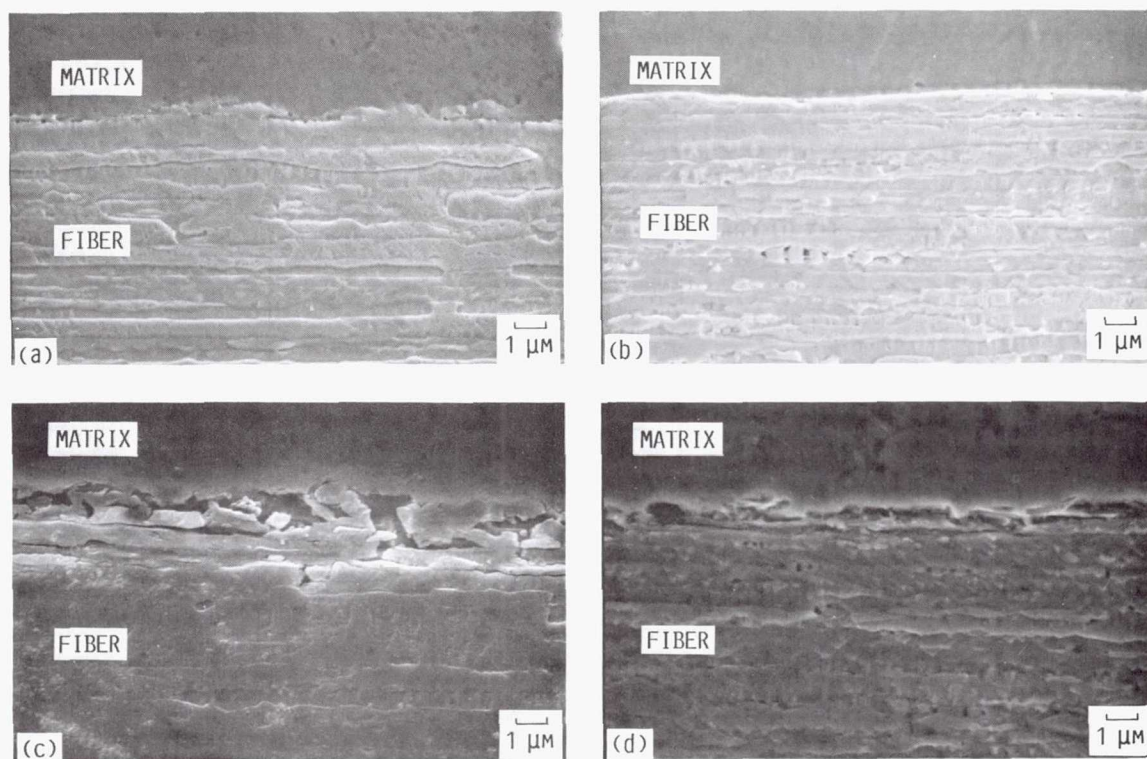


FIGURE 6. - SEM PHOTOMICROGRAPHS OF 218/Nb ((a), (c)) AND ST300/Nb ((b), (d)) (LONGITUDINAL SECTIONS), SHOWING THE DIFFERENT FIBER-MATRIX INTERACTION WITH THE EXPERIMENTAL CONDITIONS: (a) AND (b) AS-FABRICATED CONDITION, (b) AND (d) AFTER TENSILE TESTING AT 1600 K AND  $8.5 \times 10^{-4}$  MM/SEC.

a broadening of the fibrous grains after long-term (low strain rate) tensile testing at 1600 K. In comparison, no segmentation of the fibrous grains was evident after fabrication (Figs. 6(a) and (b)). Since these recrystallization phenomena, segmentation and broadening of the fibrous grains, were reported for the free wires tested at similar conditions (Ref. 6), microstructural changes observed in the fibers in the composite are not presumed to be directly caused by the presence of niobium. However, niobium diffusion into the fiber may have enhanced the recrystallization kinetics near the fiber surface.

The tungsten fiber surface and the interface zone between tungsten and niobium were revealed by etching for tungsten. The 218/Nb interface zone had nearly the same fibrous grain structure as the bulk fiber but was severely cracked during testing (Fig. 6(c)). The ST300/Nb interface zone did not display severe cracking (Fig. 6(d)). The reason for the difference between the two composites is not fully understood. This difference in interface cracking tendency may be due to differences in wire fabrication techniques, surface chemistry, surface roughness and composition. Generally, metallographic examination of transverse and longitudinal sections indicate that the thickness of the interface zone increased as the testing temperature increased and as the initial crosshead speed decreased. The thickness of the interface zone also appeared to be influenced by the same factors that affected the interface cracking tendency. After tensile testing at 1600 K at a crosshead speed of  $8.5 \times 10^{-4}$  mm/sec, the interface zone in the 218/Nb (Fig. 7(b)) was thicker than that in ST300/Nb (Fig. 7(a)). X-ray microprobe analysis was conducted on the transverse section of these two composites (Figs. 7(c) and (d)). However, the interdiffusional profiles of tungsten and niobium suggest that the two tungsten fibers had the same interface zone chemistry and the same relative depth into the matrix. The difference in the composition profiles, if any, between the two composites

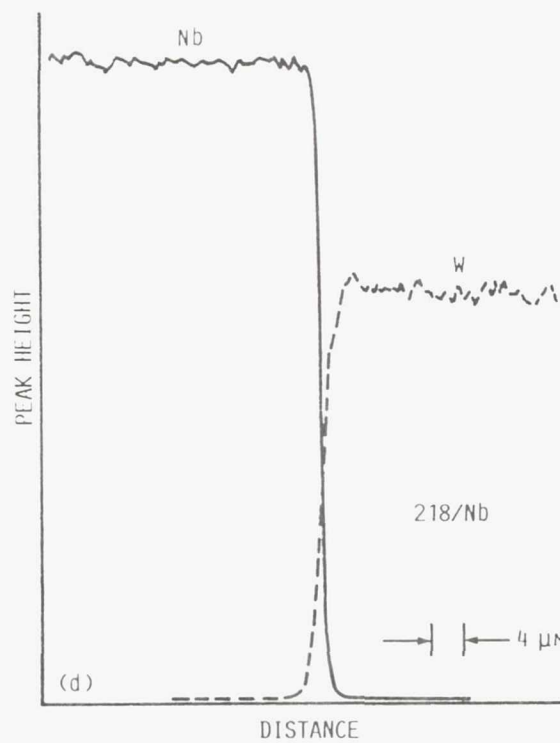
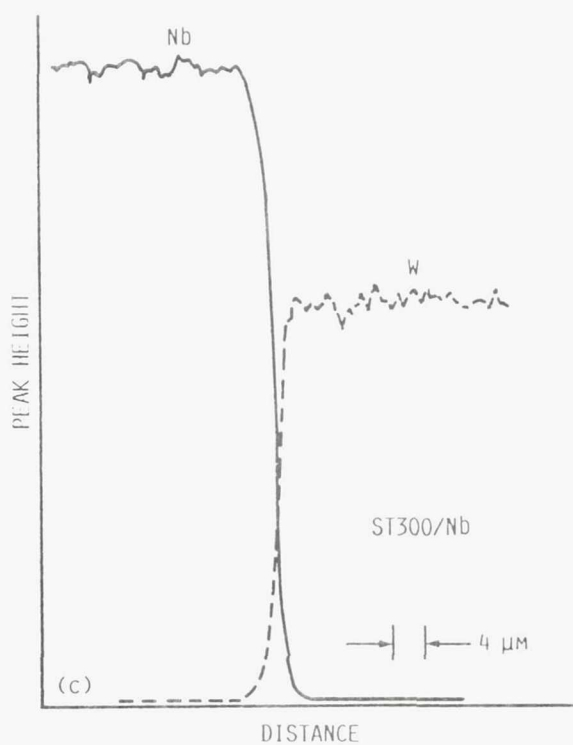
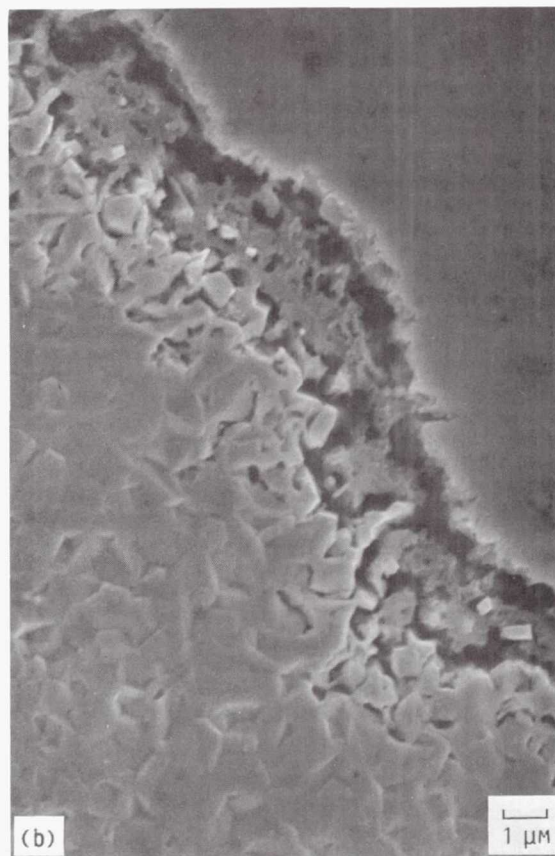
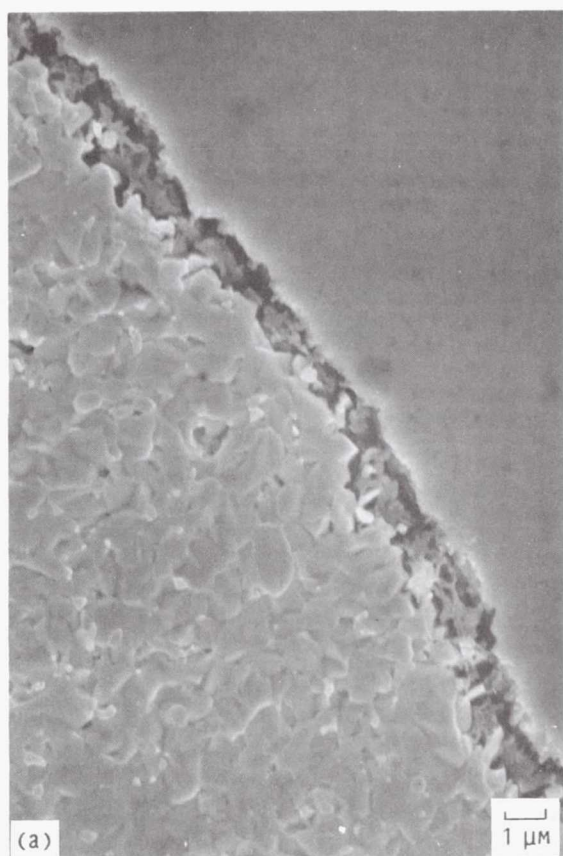


FIGURE 7. - SEM MICROGRAPHS (TRANSVERSE SECTIONS OF ST300/Nb (a) AND 218 Nb (b), AND X-RAY MICRO PROBE PROFILES OF W AND Nb IN ST300/Nb (c) AND 218/Nb (d) AFTER TENSILE TESTING AT 1600 K AND A CROSSHEAD SPEED OF  $8.5 \times 10^{-4}$  MM/SEC.

interface zones likely occurs below the resolution range of the x-ray microprobe. Since the high-temperature, long-term tensile tested specimens showed a negligible interdiffusion depth (less than  $4\text{ }\mu\text{m}$ ), other short-term tensile tested specimens are assumed to have the same or less interdiffusion. The effect of solid-solution strengthening in the niobium matrix or weakening of the tungsten fiber induced by niobium would be too small to be of consequence considering that only 3 percent of the fiber and matrix volume is affected.

The microstructures of the niobium matrix in the composite and in the arc sprayed monolithic niobium sheet are shown in Fig. 8. Both showed homogeneous structures. In the composites, however, the grain size of the Nb adjacent to the fiber interface was much finer than the grain size of the bulk Nb. It is believed that this fine grain size is due to restricted grain growth during the composite consolidation.

#### Composite Fracture Behavior

The reduction of area (RA) was measured on fractured tensile specimens. Figure 9 shows the measured RA of 218/Nb, ST300/Nb, 218, ST300 and monolithic Nb as a function of crosshead speed at 1600 K. In comparison to the composite, the arc sprayed monolithic Nb showed a higher RA and a negative strain rate dependency, i.e., a higher RA at the low crosshead speed than at the high crosshead speed. The RA of composites with both types of fiber decreased from 40 percent at high crosshead speeds to below 10 percent at low crosshead speeds. The decrease of RA is attributed to embrittlement and lower ductility of the fiber due to segmentation and broadening of fibrous grain structures in the tungsten fiber. At 1300 to 1500 K the composites also showed nearly a 40 percent RA. The RA behavior of the 218 and ST300 wires (Ref. 6) shows similar behavior to that of the composites.

Figure 10 shows a fracture surface of 218/Nb and ST300/Nb composite tensile specimens tested at a low crosshead speed at 1600 K. The longitudinal sections are shown in (a) and (b), and the corresponding fracture surfaces (c) and (d). Both types of fiber exhibited brittle fracture without necking. The longitudinal section of the ST300/Nb composite interface showed few voids and no indication of delamination between fiber and matrix at fracture. The interface of 218/Nb composite, however, exhibited numerous voids and evidence of delamination between the fiber and matrix at fracture. The fracture surface of the composite interface region was different, i.e.,

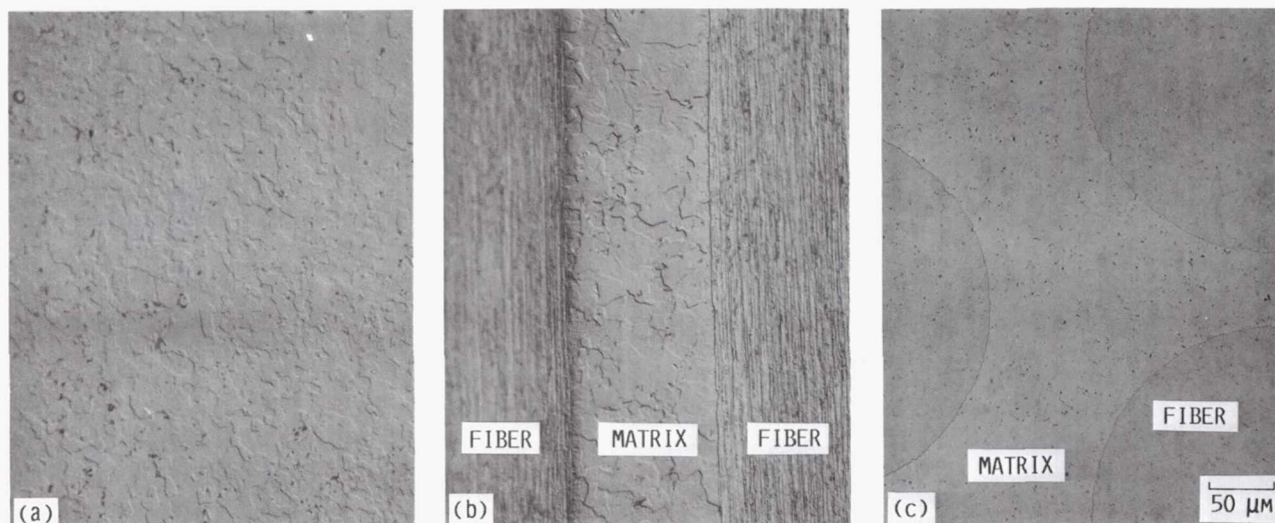


FIGURE 8. - LIGHT MICROSCOPE GRAIN STRUCTURES OF ARC-SPRAYED AND HIPED NIOBIUM (a), ARC-SPRAYED AND HIPED ST300/Nb, LONGITUDINAL SECTION (b), AND TRANSVERSE SECTION (c).

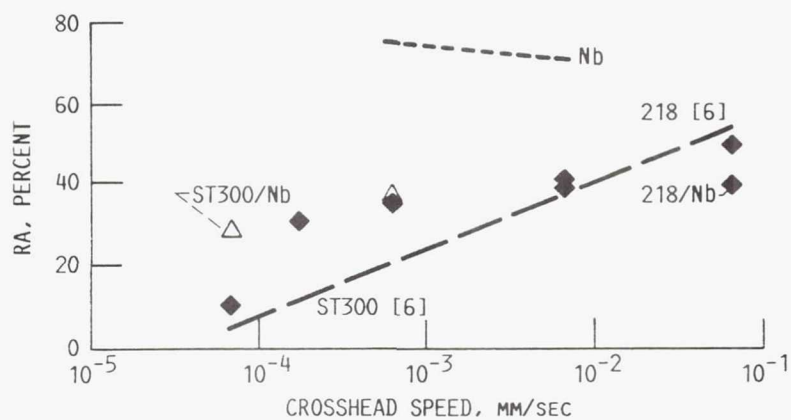


FIGURE 9. - REDUCTION OF AREA (RA) OF 218, ST300, 218/Nb, ST300/Nb AND Nb TENSILE TESTED AT 1600 K AS A FUNCTION OF CROSSHEAD SPEED.

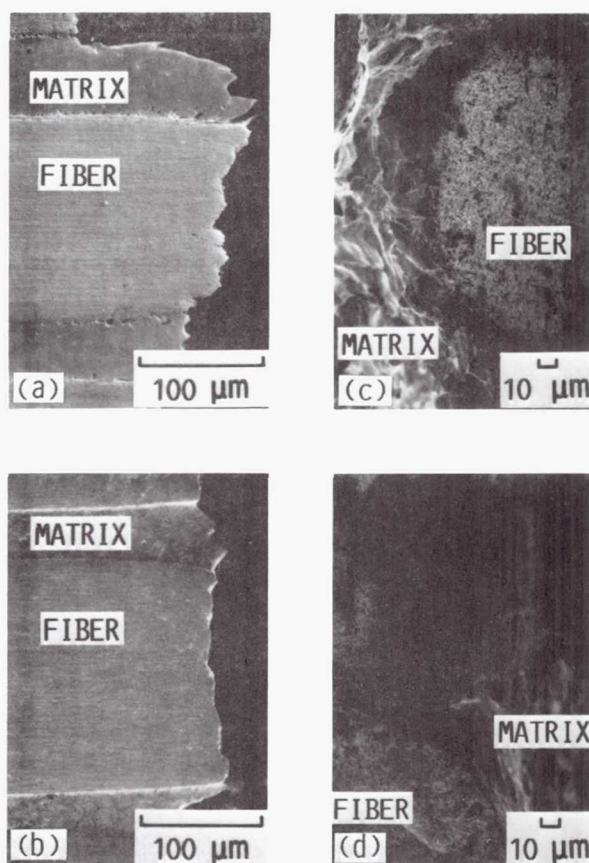


FIGURE 10. - COMPARISON OF FRACTURE MORPHOLOGY BETWEEN 218/Nb AND ST300/Nb, TENSILE TESTED AT 1600 K AND  $8.5 \times 10^{-4}$  MM/SEC.

- (a) LONGITUDINAL SECTION OF 218/Nb.
- (b) LONGITUDINAL SECTION OF ST300/Nb.
- (c) FRACTURE SURFACE OF 218/Nb.
- (d) FRACTURE SURFACE OF ST300/Nb.

the ST300/Nb interface exhibited a ductile facet fracture with some cracks propagating through the matrix, whereas the 218/Nb interface appeared to be brittle with cracks propagating along the interface.

### Discussion

#### Deviation of Tensile Behavior from the Rule-of-Mixtures

With the known constituent tensile properties of the free fiber and monolithic matrix, the composite tensile strength may be estimated using the rule-of-mixtures (ROM) (Refs. 7 and 8):

$$\sigma_C = \sigma_f V_f + \sigma_m V_m \quad (1)$$

$$V_f + V_m = 1$$

where  $\sigma_C$ ,  $\sigma_f$ ,  $\sigma_m$  are the strengths of the composite (c), the fiber (f), and the matrix (m) at a constant strain. The volume fraction of each component is represented by  $V_f$  and  $V_m$  respectively. Figure 11 schematically shows the tensile curves of the matrix, composite, and fiber at a constant temperature and demonstrates how the tensile stress ( $\sigma_{PL}$ ) of each component is determined. The tensile behavior of the fiber and composite are similar in terms of the yield point and the fracture point and differ only in the amount of stress required. Yielding of the matrix in the W/Nb composite system occurs earlier than that of the fiber and the composites because of its smaller elastic region (Fig. 2). Since strain hardening of niobium is negligible at temperatures of 1300 to 1600 K, we assume that the value of the proportional limit of the matrix is equal to its stress contribution at the composite yield point. Therefore, the value of the proportional limit of the composite,  $\sigma_{PL}$ , can now be calculated using the following ROM relationship:

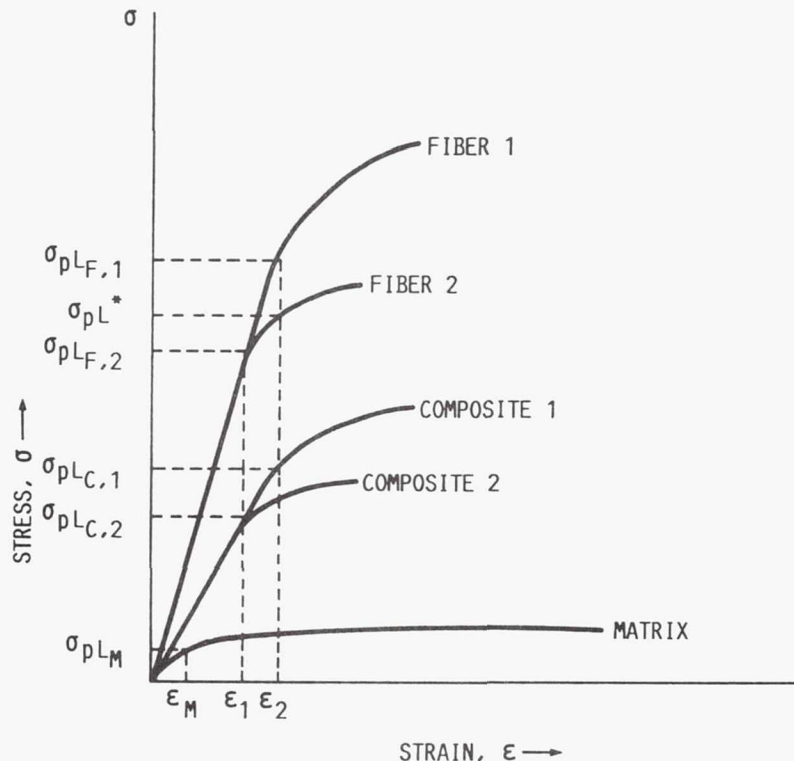


FIGURE 11. - SCHEMATIC STRESS-STRAIN CURVE OF MATRIX, COMPOSITE AND FIBER FOR THE ROM CALCULATION.

$$(\sigma_{PL})_C = (\sigma_{PL})_f V_f + (\sigma_{PL})_m V_m \quad (2)$$

where  $(\sigma_{PL})_m$  is the matrix strength at a strain of  $(\sigma_{PL})_f$ .

Temperature influence. The experimental and calculated  $\sigma_{PL}$  of the composites as a function of temperature are shown in Fig. 12. The  $\sigma_{PL}$  for 218/Nb composites calculated using the ROM is in good agreement with the measured values. The  $\sigma_{PL}$  deviation of the composites is defined as the difference between the experimentally measured and the calculated  $\sigma_{PL}$ , ( $D = (\sigma_{PL})_{exp} - (\sigma_{PL})_{cal}$ ). The deviation direction for the 218/Nb composites was affected by test temperature: at low temperatures the experimental value was higher (positive deviation) than the calculated, but at high temperatures it was lower (negative deviation) than the calculated. The experimentally determined  $\sigma_{PL}$  of ST300/Nb composites at 1500 and 1600 K displayed a considerable positive deviation from the calculated values, about 90 MPa at 1500 and about 70 MPa at 1600 K. A similar positive deviation, about 130 MPa, was previously observed at 1366 K (Ref. 5).

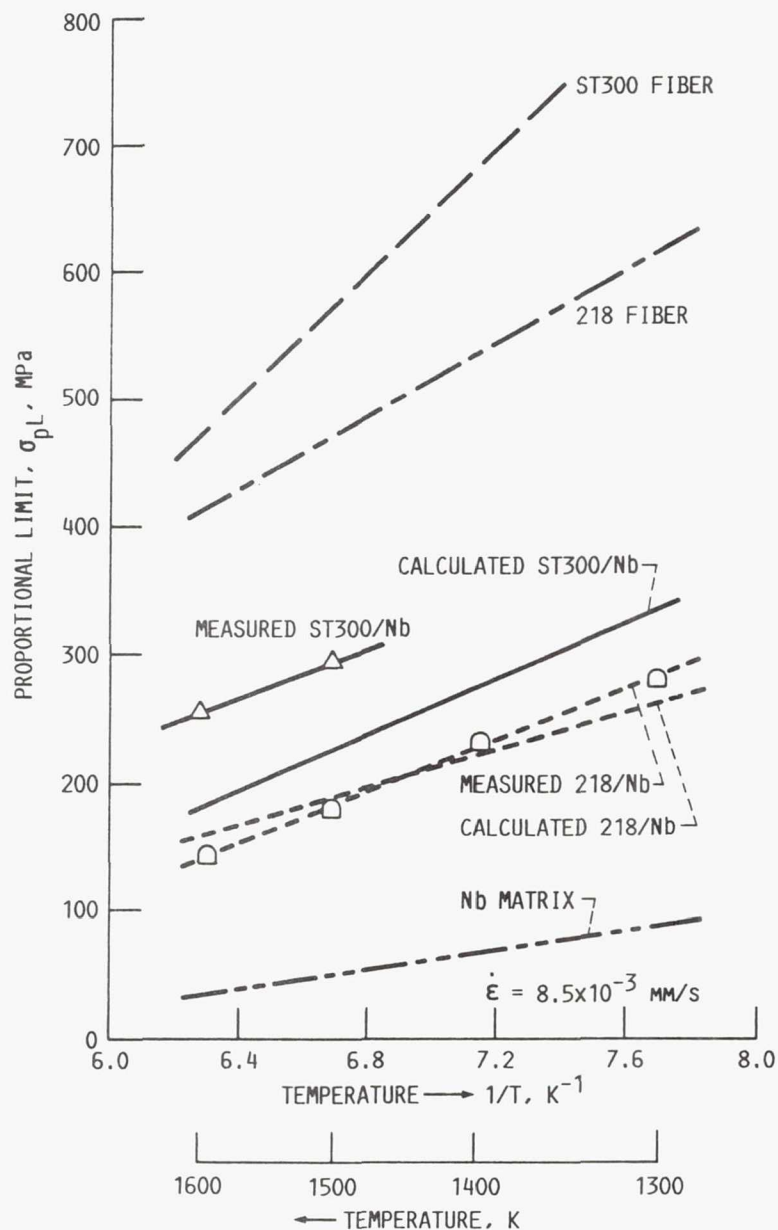


FIGURE 12. - DEVIATION OF COMPOSITE TENSILE STRENGTH FROM THE ROM CALCULATION AS FUNCTIONS OF TEMPERATURE AND FIBER COMPOSITION.

## Causes of ROM Deviations

Experimental variables. In order to understand the deviation from the ROM calculations of the composite tensile properties, the extent of the experimental errors was investigated. Voids and poor bonding in the interface zone, fiber misalignment, and fiber breakage were not observed in this system, and were not considered to be a source of error.

The constituent fiber tensile properties and fiber volume fraction are possible sources of error. Each composite sheet specimen examined contained as many as 77 continuous fibers in the gauge section, and fluctuations in the tensile properties of each fiber may cause an error. However, the tensile strength of individual tungsten alloy fibers was found to have a negligibly small fluctuation at high temperatures. For example, the scatter range in tensile strength was about +15 MPa or about +4 percent for a  $\sigma_{PL}$  of 350 MPa at 1600 K for 10 randomly chosen ST300 samples from different spools and winding positions within a spool. Table II shows the  $\sigma_{PL}$  values of the as-drawn ST300 wires. The scatter range in the tensile strength of the 218 fiber was assumed to be equivalent to that of the ST300 fiber. A decrease in fiber tensile strength during the composite fabrication is discounted because of the relatively low fabrication temperatures (Refs. 5 and 6) compared with the melting point of the fiber and the short fabrication time at temperature.

The ROM calculations were made using composite fiber tensile properties of electropolished as-drawn fibers. These fibers provided a fiber tensile specimen with a 25.4 mm gauge section, equivalent to the composite specimens, and were reported to have a tensile strength of 450 MPa at 1600 K, about 100 MPa more than that of the unpolished as-drawn fibers (Ref. 6). This difference would cause a negative deviation from the ROM of as much as 32 MPa for a fiber volume fraction of 0.33, since the composites were made using unpolished as-drawn wires.

Fluctuations in the fiber diameter may also affect the composite tensile strength. The normalized composite tensile strength with respect to a constant volume fraction was calculated, based on the simple linear relationship of  $\sigma_C = AV_f$  (Refs. 8 and 9), where  $A$  is a constant,  $V_f$  the fiber

TABLE II. - FLUCTUATION OF THE  $\sigma_{PL}$  OF  
ST300 WIRES (AS-DRAWN/UNPOLISHED) AT  
1600 K AND AT  $8.5 \times 10^{-3}$  mm/sec

Spool number	Position number	Wire diameter, $\mu\text{m}$	$\sigma_{PL}$ , MPa
201 ↓	1	201	347.8
	2	201	330.3
	3	198	334.6
	4	203	353.6
	5	198	348.6
110	1	193	379.1
111	2	198	337.6
101	1	206	339.0
101	2	198	341.5
102	1	203	381.6

volume fraction, and  $\sigma_C$  the composite tensile strength. For instance, for  $V_f = 0.33$  with an error of 0.04 ( $V_f = V_f(1 - (d/d_0)^2)$ , where  $V_f$  is an error range at  $V_f = 0.33$ ,  $d_0 = 200 \mu\text{m}$ ,  $d = 187$  to  $213 \mu\text{m}$ ) due to the fiber diameter variation, the normalized experimental value for composites with  $\sigma_C = 250 \text{ MPa}$  could vary from 280 to 220 MPa. The error of 0.04 in  $V_f$  results from the possible wire diameter fluctuation of  $+13 \mu\text{m}$  on a  $200 \mu\text{m}$  nominal fiber diameter. The effect of possible errors in the deviation is summarized in Table III. The summation of all errors accounted for is about  $+3/-66 \text{ MPa}$ . This error does not explain the observed positive deviation (over 70 MPa) from the ROM predictions.

Fiber/matrix interaction. The deviation from the ROM may be partially attributed to the rheological interaction and the chemical interdiffusion which takes place between the fiber and the matrix. The formation of the W-Nb alloy interface zone implies a effective constraining of fiber materials. Lee et al. (Ref. 9) reported that a finer grain size was found in the W/Cu composite fabricated by the Cu infiltration process, and that this fine grain size caused an increase in the matrix strength contribution. On the other hand, the interdiffusion of niobium into the tungsten fiber lowers the recrystallization temperature of the tungsten and results in a reduction in fiber strength. Matrix strengthening or fiber strength degradation would result in positive and negative deviations, respectively. In order to better explain the deviation from the ROM, the  $\sigma_m$  and  $\sigma_f$  terms of the ROM were modified to incorporate residual stress, mean stress, and interdiffusion-induced fiber degradation as follows:

(1) Residual Stress Effect: Due to the coefficient of thermal expansion mismatch ( $6.8 \times 10^{-6}$  for Nb and  $4.3 \times 10^{-6} \text{ K}^{-1}$  for W at room temperature, and  $10.3 \times 10^{-6}$  for Nb and  $4.8 \times 10^{-6} \text{ K}^{-1}$  for W at 1500 K), an axial tensile residual stress may form in the matrix near the fiber during the composite fabrication and could cause some matrix yielding upon cool down to room temperature (Ref. 3). This kind of positive residual stress has been reported to lower the composite's flow stress (Ref. 10). High temperature tensile testing results in an additional thermal cycle on the composite specimens. The tensile strength was measured during a heating cycle, and the microstructure was observed after cooling. It is known that a compressive stress in the matrix near the fiber is formed when a composite with this type of thermal expansion mismatch between the fiber and matrix is heated after a cooling cycle (Refs. 11 and 12).

TABLE III. - ESTIMATED DEVIATIONS FROM THE ROM  
CALCULATION FOR W/Nb COMPOSITES TESTED AT 1600 K

Error source	Error range, MPa	Effect on the deviation with $V_f = 0.33$ , MPa
Fiber strength	15	4.5
Electro-polishing	100	32
Volume fraction of fiber	30	30

If we make the assumption that the compressive residual stress is not fully relaxed, the compressive stress may cause matrix yielding, and the amount of negative plastic strain would increase with increasing temperature. When loaded in tension under this condition for high temperature tensile tests, the direction of the moving dislocations on a slip plane must change, and this change requires a stress. This additional stress is a function of the negative plastic strain, which is a negative creep strain in the presence of a compressive stress at high temperatures for niobium. This internal stress would cause a higher matrix contribution to the composite tensile strength. This matrix contribution could be expected to decrease with decreasing strain rate. As an analog, Arsenault et al. (Ref. 13) reported that the compressive strength of SiC<sub>w</sub>/Al composites was higher than the tensile strength because of a tensile residual stress upon compressive loading at room temperature.

To mathematically modify the matrix stress contribution of the present composites, the internal stress caused by the compressive residual stress and the negative plastic strain were estimated. To change the flow direction of dislocations, the necessary stress would be roughly the flow stress of niobium. The niobium matrix strengthening,  $\Delta\sigma_m$ , is assumed to be a function of the residual compressive stress, i.e.,

$$\Delta\sigma_m = \sigma_{m, \text{tensile}} \quad (3)$$

where  $\sigma_{m, \text{tensile}}$  is the tensile flow stress. In Table IV, the estimated  $\Delta\sigma_m$  and the composite flow stress,  $\sigma_c^*$ , are recalculated by the equation,

$$\sigma_c^* = (\sigma_{m, \text{tensile}} + \Delta\sigma_m)(1 - V_f) + \sigma_f V_f \quad (4)$$

The calculated  $\Delta\sigma_m$  of niobium varied from 39 to 93 MPa, depending on the flow stress. The contribution from  $\Delta\sigma_m$  resulted in a nearly doubled matrix stress contribution. The corresponding  $\sigma_c^*$  appeared to be much higher than  $\sigma_c^{\text{exp}}$  or  $\sigma_c^{\text{ROM}}$ , particularly for 218/Nb. On the other hand,  $\sigma_c^*$  for ST300/Nb was not high enough to explain the measured  $\sigma_c^{\text{exp}}$ . The calculated  $\sigma_c^*$  was nearly 40 MPa less than the experimental value, but the  $\sigma_c^*$  values were closer to experimental than were the values calculated without the stress contribution.

The modification of the ROM in terms of the simple compressive residual stress does not appear adequate for both the 218/Nb and ST300/Nb

TABLE IV. - RESIDUAL STRESS EFFECT ON THE HIGH TEMPERATURE TENSILE PROPERTIES AT INITIAL CROSSHEAD SPEED OF  $8.5 \times 10^{-3}$  mm/sec

Material	Temperature, K	$\sigma_c^{\text{exp}}$ , MPa	$\sigma_c^{\text{ROM}}$ , MPa	$\Delta\sigma_m$ , MPa	$\sigma_c^*$ , MPa
218/Nb	1300	278.0	265.8	92.6	327.8
	1400	232.9	229.7	78.1	272.9
	1500	174.2	187.9	59.9	227.1
	1600	150.3	158.0	38.7	183.9
ST300/Nb	1500	293.0	220.4	59.9	260.1
	1600	252.1	179.8	38.7	205.7

composites. It would appear that a strong fiber is more effective for matrix strengthening than a weak fiber, and that fiber strength has more than a linear effect on matrix strengthening.

(2) Mean Stress Effect: In analyzing the effect of the mean stress on matrix strengthening, the composite is assumed to be a system, in which the niobium matrix possesses a hard second phase of tungsten fibers. When a tensile load is applied at high temperatures, the niobium matrix deforms plastically, while the tungsten fibers deform elastically. A moving dislocation would be blocked by the fibers; that is, the deformation of niobium would be impeded by the elastic response of the fibers. This impeding stress to plastic flow was calculated by Brown et al. (Refs. 14 and 15). Analysis of continuous tungsten-copper composites as a function of fiber diameter (Ref. 4) shows that Brown's mean stress was higher than Orowan's stress for relatively large diameter fibers (15  $\mu\text{m}$ ).

In this study, niobium is strengthened by the mean stress, which is simply proportional to fiber volume fraction and to the accumulated plastic strain (Ref. 15). The niobium matrix strengthening term  $\sigma_{M,m}$  is given by the following relationship,

$$\sigma_{M,m} = \frac{2K\varepsilon_p G_f G_m V_f}{G_f - K(G_f - G_m)} \quad (5)$$

where  $K$  is an accommodation factor between fiber and matrix, and  $\varepsilon_p$  is the accumulated plastic strain or the work hardening parameter and is a direct function of the elastic response of the fibers and the plastic behavior of matrices. The continuous fiber component carries the applied load due to its volume fraction, and the ROM may be modified by the matrix strengthening term with  $\sigma_{M,m}$  of Eq. (5), such that the composite strength  $\sigma_C^*$  is calculated using the following equation,

$$\sigma_C^* = \sigma_f V_f + \sigma_m (1 - V_f) + \sigma_{M,m} (1 - V_f) \quad (6)$$

A fiber with a higher yield point as depicted in Fig. 11 will result in a higher plastic strain in the matrix than a fiber with a lower yield point with the same fiber elastic modulus. This means the fiber with the higher yield point will possess a higher  $\varepsilon_p$ . At the yield point of the composite,  $\varepsilon_p$  will be the elastic strain difference between the fiber and matrix,

$$\varepsilon_p = A \left[ \frac{(\sigma_{PL})_f}{2G_f} - \frac{(\sigma_{PL})_m}{2G_m} \right] \quad (7)$$

where  $A$  is a constant, which can depend upon possible strain relaxation (Ref. 16), and  $G_f$  and  $G_m$  are the shear modulus of the fiber and matrix, respectively. For instance, at 1600 K,  $\sigma_{M,m}$  and  $\varepsilon_p$  can be roughly estimated with  $K = 0.78$  (Ref. 14) in Eq. (5) and  $A = 1$  in Eq. (7) with no strain relaxation. For this first approximation, the strain relaxation at the low strain rate was neglected. In Table V the estimated values of  $\varepsilon_p$  and  $\sigma_{M,m}$  and  $\sigma_C^*$ , modified by the mean stress were summarized for both composites. The work hardening parameter,  $\varepsilon_p$ , increases with increasing  $\sigma_{PL}$  of the fiber and results in a higher mean stress. This effect means that a high mean stress will exist when the  $\sigma_{PL}$  is raised by the higher strength fiber. An increased strain rate caused a higher  $\sigma_{PL}$  in tungsten fibers (Ref. 6), and the general positive deviation of ST300/Nb and 218/Nb at high crosshead speed could be caused by a high mean stress. The  $\sigma_C^*$

TABLE V. - MEAN STRESS EFFECT ON THE ROM  
AT 1600 K AND VARIOUS CROSSHEAD SPEEDS

Composite	Crosshead speed, mm/sec	$\sigma_C^{\text{exp}}$ , MPa	$\sigma_{M,m}$ , MPa	$\sigma_C^*$ , MPa	$\sigma_C^{\text{ROM}}$ , MPa	$\epsilon_p$ , mm/mm
218/Nb	$8.5 \times 10^{-2}$	180.1	45.3	211.2	180.6	$8.1 \times 10^{-4}$
	$8.5 \times 10^{-4}$	102.0	35.7	143.7	119.8	$6.4 \times 10^{-4}$
ST300/Nb	$8.5 \times 10^{-2}$	295.3	51.3	229.5	195.1	$9.2 \times 10^{-4}$
	$8.5 \times 10^{-4}$	160.4	38.0	151.0	125.5	$6.8 \times 10^{-4}$

was affected by the different mean stress at the various crosshead speeds: i.e., 144 and 211 MPa for 218/Nb at low crosshead speeds and high crosshead speeds, respectively. This increase of  $\sigma_C^*$  is again higher than the measured values of 102 and 180 MPa at low and high crosshead speeds, respectively. The  $\sigma_C^*$  of ST300/Nb, 229 MPa at a high crosshead speed, is higher than that of  $\sigma_C^{\text{ROM}}$ , 195 MPa, but still lower than that of the measured value of 295 MPa.

(3) Combined Stress Effect: Figure 13 illustrates the modified ROM calculation for ST300/Nb composites at 1600 K, based on the matrix strengthening by both the residual stress effects and the mean stress effects, assuming no stress relaxation occurs. The effect of the two-stresses were included in the ROM calculation using Eqs. (4) and (6). At low crosshead speeds the modified ROM calculation for the  $\sigma_{PL}$  of ST300/Nb composite slightly exceeded the measured value, but at a high crosshead speed the calculated values were still lower than the measured ones. The first approximation for the residual and mean stress calculation is believed to be overestimated, in particular at the low crosshead speeds, since the accumulated stresses would probably relax in the Nb matrix at 1600 K. The increase in the calculated composite tensile strength at high crosshead speeds is believed to be too high, because this would require that the strength of the matrix increase from about 40 to 130 MPa (Fig. 13). Such a large increase is not believed to be realistic.

Matrix strengthening alone does not explain the higher composite tensile strength of the ST300/Nb. The interfacial bonding between fiber and matrix may alter the strain on the fiber at the proportional limit as well as the strain on the fiber at UTS. For example, a strong ductile fiber/matrix bond would cause the composite to yield later than the free fiber (Fig. 11). The delayed yielding of the composite (e.g., ST300/Nb) may possibly be due to an increase in the proportional limit of the fiber caused by the passive effect that the interface has in reducing imperfections in the fiber surface.

Another possible cause of the delayed composite yielding may be differences in the instantaneous strain behavior of the matrix and the fiber in the composite. A larger degree of matrix deformation may result in greater plastic fiber deformation in this case where the fiber/matrix bond is very strong and ductile. The different amounts of deformation must be balanced to get a homogeneous strain distribution across the fiber/matrix interface. Composite yielding, then, may occur at a larger strain value than the free fiber yield point, as in Fig. 11 where the free fiber yields at  $\epsilon_1$ , but

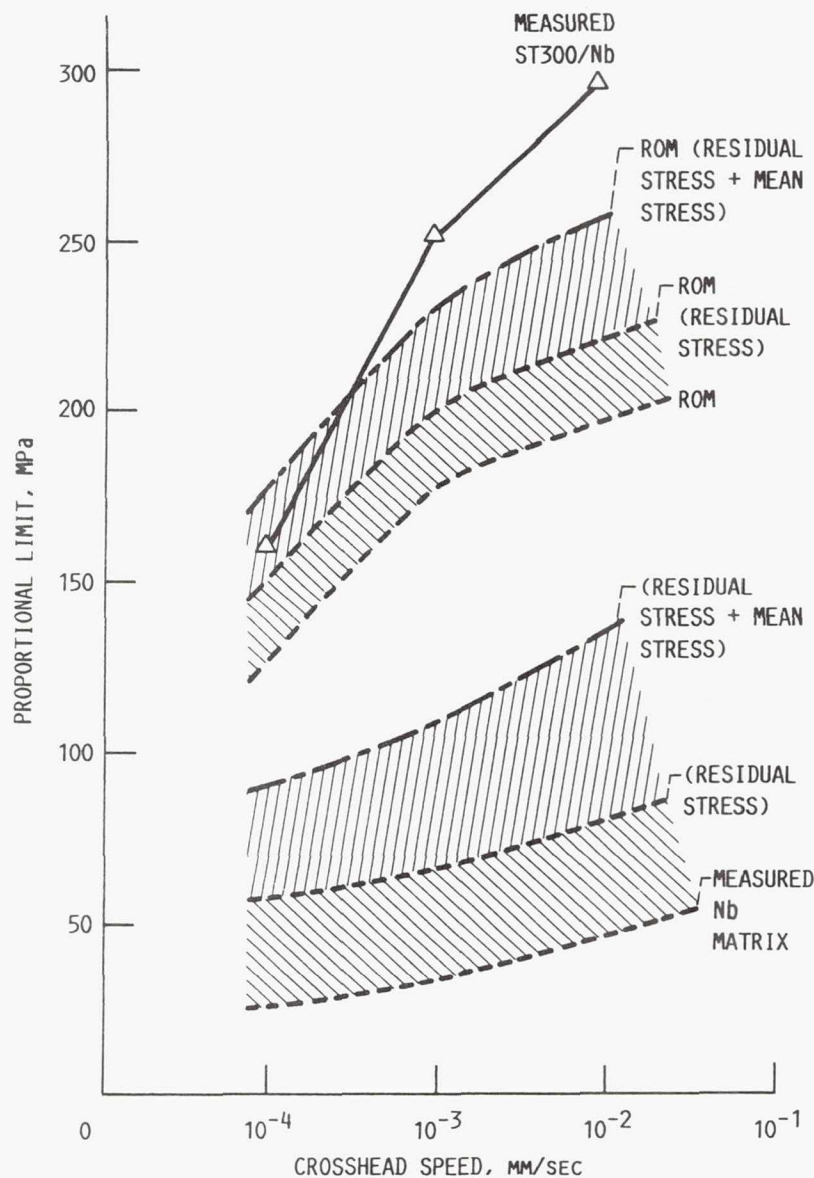


FIGURE 13. - CALCULATED  $\sigma_{PL}$  (EQS. (4) AND (6)) OF ST300/Nb COMPOSITE AS A FUNCTION OF CROSSHEAD SPEED, BASED ON THE RESIDUAL AND MEAN STRESSES IN THE Nb MATRIX AT 1600 K.

its composite yields at  $\epsilon_2$ . This would appear to be fiber strengthening because the fiber strength contribution at the composite yield point appears higher than the  $\sigma_{PL}$  of the free fiber, i.e.,  $\sigma_{PL}^*$  instead of  $\sigma_{PL,f2}$  (Fig. 11). Hence, the importance of characterizing the very thin interface zone is seen, but is, unfortunately, beyond the scope of this study. The possible difference in quality of the diffusion bond between the fiber and matrix due to different dispersoids in the two fibers may also contribute to the observed deviation from the ROM. The difference in the fiber/matrix bond may also depend on the fiber surface finish due to drawing processes and cleaning procedures used during fiber fabrication.

Fiber degradation. Fiber degradation can result in composite strengths lower than the ROM predictions (Ref. 8). This degradation can be caused by the formation of an interface zone and matrix-element-induced weakening of bulk fiber (e.g., niobium-induced tungsten-fiber recrystallization). A slightly larger recrystallized interface zone was observed in the 218/Nb than in the ST300/Nb composite. The interface zone is believed to possess

a lower tensile strength than the tungsten fiber, and the cracked interface observed in the 218/Nb composite could cause a premature failure of the fiber component. These mechanisms could account for the lower fracture strain of 218/Nb (about 10 percent) compared with ST300/Nb (about 14 percent) at 1600 K as shown in Fig. 2.

Possible fiber degradation due to the presence of niobium in tungsten is believed to be minor for these tensile tested specimens. Observed niobium diffusion into the fiber beyond the interface zone was negligible, therefore, niobium-induced recrystallization did not occur throughout the tungsten fiber, only in the reaction zone. In addition, an interface zone thickness of about 5  $\mu\text{m}$  is not expected to cause a significant strength loss when compared to the original 200  $\mu\text{m}$  fiber diameter. The 5  $\mu\text{m}$  zone results in a fiber diameter reduction from 200 to 190  $\mu\text{m}$  which can decrease the fiber volume fraction from 0.33 to about 0.30. This change in fiber volume fraction is within the error band originally calculated for the fiber volume fraction.

### Summary

A tensile tests was carried out on unidirectional tungsten fiber reinforced niobium composites in the temperature range of 1300 to 1600 K and the results are summarized below:

1. The ST300/Nb composites were stronger than the 218/Nb composites over the entire range of temperatures.
2. The ST300/Nb composites were considerably stronger than ROM prediction, whereas the tensile strength of the 218/Nb composites fell within the calculated error of the ROM prediction.
3. The differences in the tensile behavior of the two types of composites relative to the ROM predictions is believed to be related to differences in the fiber-matrix interface zone for the two fibers.
4. The positive deviation from ROM predictions of ST300/Nb tensile properties is believed to be due to the effects of both residual stresses and Brown's mean stresses.

### Conclusion

The measured tensile strengths of continuous fiber reinforced composites can exceed predicted rule-of-mixture strengths in systems where the fibers have high tensile yield strengths and strong ductile interfacial bonding with the matrix. Further research is needed to fully understand and quantify the observed positive deviations from ROM predictions.

### References

1. A. Kelly and W.R. Tyson, "Tensile Properties of Fiber-Reinforced Metals: Copper/Tungsten and Copper/Molybdenum," J. Mech. Phys. Solids, 13 (1965) 329-333.
2. R.W. Heckel, R.Z. Zaering and H.P. Cheskis, "Optimization of the Range of Elastic Behavior on Unidirectional Composites by Prestraining," Metall. Trans., 3 (1972) 2507-2513.

3. K.K. Chawla and M. Metzger, "Initial Dislocation Distribution in Tungsten Fiber-Copper Composites," J. Mater. Sci., 7 (1) (1972) 34-39.
4. A. Kelly and H. Lilholt, "Stress-Strain Curve of a Fiber-Reinforced Composite," Philos. Mag., 20 (1969) 311-328.
5. L.J. Westfall et al., "Preliminary Feasibility Studies of Tungsten/Niobium Composites for Advanced Space Power Systems Applications," NASA TM-87248, 1986.
6. H.M. Yun, "Tensile Behavior of Tungsten and Tungsten-Alloy Wires from 1300 to 1600 K," Proceedings of the Symposium on Refractory Metals - State of the Art, (Warrendale, PA: Metallurgical Society of AIME, 1988), 49-64.
7. D.L. McDanel, R.W. Jech and J.W. Weeton, "Metals Reinforced with Fibers," Met. Prog., 78 (6) (1960) 118-121.
8. D.W. Petrasek and J.W. Weeton, "Effects of Alloying on Room Temperature Tensile Properties of Tungsten-Fiber-Reinforced Copper-Alloy Composites," Trans. Metall. Soc. AIME, 230 (5) (1964) 977-990.
9. R.E. Lee and S.J. Harris, "Matrix Strengthening in Continuous Fibre Reinforced Composites under Monotonic and Cyclic Loading Conditions," J. Mat. Sci., 9 (1) (1974) 359-368.
10. H.P. Cheskis and R.W. Heckel, "Deformation Behavior of Continuous-Fiber Metal-Matrix Materials," Metall. Trans., 1 (7) (1970) 1931-1942.
11. G. Garmong, "Elastic-Plastic Analysis of Deformation Induced by Thermal Stress in Eutectic Composites: I. Theory," Metall. Trans., 5 (10) (1974) 1974-2183.
12. A.R.T. De Silva and G.A. Chadwick, "Thermal Stresses in Fiber Reinforced Composites," J. Mech. Phys. Solids, 17 (1969) 387-403.
13. R.J. Arsenault, "The Effects of Differences in Thermal Coefficients of Expansion in SiC Whisker 6061 Aluminium Composites," ICCM-Proceedings of the Fifth International Conference On Composite Materials, ed. W.C. Harrigan, Jr., J. Strife, and A.K. Dhingra (Chatsworth, CA: Composite Specialties, Inc., 1985), 21-36.
14. L.M. Brown and D.R. Clarke, "Work Hardening due to Internal Stresses in Composite Materials," Acta Metall., 23 (7) (1975) 821-830.
15. L.M. Brown and D.R. Clarke, "The Work Hardening of Fibrous Composites with Particular Reference to the Copper-Tungsten System," Acta Metall., 25 (5) (1977) 563-570.
16. O.B. Pederson, "Residual Stresses and the Strength of Metal Matrix Composites," ICCM-Proceedings of the Fifth International Conference On Composite Materials, ed. W.C. Harrigan, Jr., J. Strife, and A.K. Dhingra (Chatsworth, CA: Composite Specialties, Inc., 1985) 1-19.

# Report Documentation Page

1. Report No. NASA TM-103727 DOE/NASA/16310-15		2. Government Accession No.		3. Recipient's Catalog No.	
4. Title and Subtitle Tensile Behavior of Tungsten/Niobium Composites at 1300-1600 K				5. Report Date	
				6. Performing Organization Code	
7. Author(s) Hee Mann Yun and Robert H. Titran				8. Performing Organization Report No. E-5961	
				10. Work Unit No. 590-13-11	
9. Performing Organization Name and Address National Aeronautics and Space Administration Lewis Research Center Cleveland, Ohio 44135-3191				11. Contract or Grant No.	
				13. Type of Report and Period Covered Technical Memorandum	
12. Sponsoring Agency Name and Address U.S. Department of Energy Office of Nuclear Energy Washington, D.C. 20545				14. Sponsoring Agency Code	
15. Supplementary Notes Final Report. Prepared under Interagency Agreement DE-AI03-86SF16310. Prepared for the Fall Meeting of the Metallurgical Society, Indianapolis, Indiana, September 30—October 6, 1989. Hee Mann Yun, Cleveland State University, Cleveland, Ohio 44115. Robert H. Titran, NASA Lewis Research Center. Responsible person, Robert H. Titran (216) 433-3198.					
16. Abstract The tensile behavior of continuous-tungsten-fiber-reinforced niobium composites (W/Nb), fabricated by an arc-spray process, was studied in the 1300 to 1600 K temperature range. The tensile properties of the fiber and matrix components as well as of the composites were measured and were compared to rule of mixtures (ROM) predictions. The deviation from the ROM was found to depend upon the chemistry of the tungsten alloy fibers, with positive deviations for ST300/Nb (i.e., stronger composite strength than the ROM) and negative or zero deviations for 218/Nb.					
17. Key Words (Suggested by Author(s)) Refractory metal; Composite; Tensile; Strain rate; Tungsten; Niobium			18. Distribution Statement Unclassified—Unlimited Subject Category 26 DOE Category UC-504		
19. Security Classif. (of this report) Unclassified	20. Security Classif. (of this page) Unclassified	21. No. of pages 22	22. Price* A03		